

STRUCTURAL HEALTH MONITORING

WITH PIEZOELECTRIC WAFER ACTIVE SENSORS

VICTOR GIURGIUTIU



TBI
G537

STRUCTURAL HEALTH MONITORING

WITH
PIEZOELECTRIC WAFER
ACTIVE SENSORS

VICTOR GIURGIUTIU
University of South Carolina



E2010002128



AMSTERDAM • BOSTON • HEIDELBERG • LONDON
NEW YORK • OXFORD • PARIS • SAN DIEGO
SAN FRANCISCO • SINGAPORE • SYDNEY • TOKYO

Academic Press is an imprint of Elsevier



Cover photos © iStockphoto
Cover design by Lisa Adamitis

Academic Press is an imprint of Elsevier
30 Corporate Drive, Suite 400, Burlington, MA 01803, USA
525 B Street, Suite 1900, San Diego, California 92101-4495, USA
84 Theobald's Road, London WC1X 8RR, UK

This book is printed on acid-free paper. ☺

Copyright © 2008, Elsevier Inc. All rights reserved.

No part of this publication may be reproduced or transmitted in any form or by any means, electronic or mechanical, including photocopy, recording, or any information storage and retrieval system, without permission in writing from the publisher.

Permissions may be sought directly from Elsevier's Science & Technology Rights Department in Oxford, UK: phone: (+44) 1865 843830, fax: (+44) 1865 853333, E-mail: permissions@elsevier.com. You may also complete your request online via the Elsevier homepage (<http://elsevier.com>) by selecting "Support & Contact" then "Copyright and Permission" and then "Obtaining Permissions."

Library of Congress Cataloging-in-Publication Data

Giurgiutiu, Victor.

Structural health monitoring with piezoelectric wafer active sensors/Victor Giurgiutiu.
p. cm.

ISBN-13: 978-0-12-088760-6 (alk. paper)

1. Structural analysis (Engineering)
2. Piezoelectric devices.
3. Piezoelectric transducers.
4. Automatic data collection systems. I. Title

TA646.G55 2007

624.1'71-dc22

2007043697

British Library Cataloguing-in-Publication Data

A catalogue record for this book is available from the British Library.

ISBN: 978-0-12-088760-6

For information on all Academic Press publications
visit our Web site at www.books.elsevier.com

Printed in the United States of America

07 08 09 10 10 9 8 7 6 5 4 3 2 1

Working together to grow
libraries in developing countries

www.elsevier.com | www.bookaid.org | www.sabre.org

ELSEVIER

BOOK AID
International

Sabre Foundation

To My Loving and Understanding Family

CONTENTS

1	INTRODUCTION	1
1.1	Structural Health Monitoring Principles and Concepts,	1
1.2	Structural Fracture and Failure,	3
1.3	Improved Diagnosis and Prognosis Through Structural Health Monitoring,	7
1.4	About this Book,	10
2	ELECTROACTIVE AND MAGNETOACTIVE MATERIALS	13
2.1	Introduction,	13
2.2	Piezoelectricity,	14
2.3	Piezoelectric Phenomena,	21
2.4	Perovskite Ceramics,	23
2.5	Piezopolymers,	32
2.6	Magnetostrictive Materials,	34
2.7	Summary and Conclusions,	36
2.8	Problems and Exercises,	37
3	VIBRATION OF SOLIDS AND STRUCTURES	39
3.1	Introduction,	39
3.2	Single Degree of Freedom Vibration Analysis,	39
3.3	Vibration of Continuous Systems,	64
3.4	Summary and Conclusions,	98
3.5	Problems and Exercises,	98
4	VIBRATION OF PLATES	101
4.1	Elasticity Equations for Plate Vibration,	101
4.2	Axial Vibration of Rectangular Plates,	101
4.3	Axial Vibration of Circular Plates,	104
4.4	Flexural Vibration of Rectangular Plates,	110
4.5	Flexural Vibration of Circular Plates,	117
4.6	Problems and Exercises,	128

5	ELASTIC WAVES IN SOLIDS AND STRUCTURES	129
5.1	Introduction, 129	
5.2	Axial Waves in Bars, 130	
5.3	Flexural Waves in Beams, 148	
5.4	Torsional Waves in Shafts, 161	
5.5	Plate Waves, 162	
5.6	3-D Waves, 172	
5.7	Summary and Conclusions, 181	
5.8	Problems and Exercises, 182	
6	GUIDED WAVES	185
6.1	Introduction, 185	
6.2	Rayleigh Waves, 186	
6.3	SH Plate Waves, 190	
6.4	Lamb Waves, 198	
6.5	General Formulation of Guided Waves in Plates, 222	
6.6	Guided Waves in Tubes and Shells, 224	
6.7	Guided Waves in Composite Plates, 228	
6.8	Summary and Conclusions, 237	
6.9	Problems and Exercises, 238	
7	PIEZOELECTRIC WAFER ACTIVE SENSORS	239
7.1	Introduction, 239	
7.2	PWAS Resonators, 241	
7.3	Circular PWAS Resonators, 263	
7.4	Coupled-Field Analysis of PWAS Resonators, 274	
7.5	Constrained PWAS, 278	
7.6	PWAS Ultrasonic Transducers, 288	
7.7	Durability and Survivability of Piezoelectric Wafer Active Sensors, 300	
7.8	Summary and Conclusions, 306	
7.9	Problems and Exercises, 306	
8	TUNED WAVES GENERATED WITH PIEZOELECTRIC WAFER ACTIVE SENSORS	309
8.1	Introduction, 309	
8.2	State of the Art, 310	
8.3	Tuned Axial Waves Excited by PWAS, 312	
8.4	Tuned Flexural Waves Excited by PWAS, 316	
8.5	Tuned Lamb Waves Excited by PWAS, 321	
8.6	Experimental Validation of PWAS Lamb-Wave Tuning in Isotropic Plates, 330	
8.7	Directivity of Rectangular PWAS, 339	
8.8	PWAS-Guided Wave Tuning in Composite Plates, 347	
8.9	Summary and Conclusions, 360	
8.10	Problems and Exercises, 361	

9	HIGH-FREQUENCY VIBRATION SHM WITH PWAS MODAL SENSORS – THE ELECTROMECHANICAL IMPEDANCE METHOD	363
9.1	Introduction, 363	
9.2	1-D PWAS Modal Sensors, 367	
9.3	Circular PWAS Modal Sensors, 380	
9.4	Damage Detection with PWAS Modal Sensors, 388	
9.5	Coupled-Field FEM Analysis of PWAS Modal Sensors, 427	
9.6	Summary and Conclusions, 432	
9.7	Problems and Exercises, 433	
10	WAVE PROPAGATION SHM WITH PWAS	435
10.1	Introduction, 435	
10.2	1-D Modeling and Experiments, 446	
10.3	2-D PWAS Wave Propagation Experiments, 461	
10.4	Pitch-Catch PWAS-Embedded NDE, 468	
10.5	Pulse-Echo PWAS-Embedded NDE, 474	
10.6	PWAS Time Reversal Method, 481	
10.7	PWAS Passive Transducers of Acoustic Waves, 496	
10.8	Summary and Conclusions, 500	
10.9	Problems and Exercises, 501	
11	IN-SITU PHASED ARRAYS WITH PIEZOELECTRIC WAFER ACTIVE SENSORS	503
11.1	Introduction, 503	
11.2	Phased-Arrays in Conventional Ultrasonic NDE, 505	
11.3	1-D Linear PWAS Phased Arrays, 507	
11.4	Further Experiments with Linear PWAS Arrays, 518	
11.5	Optimization of PWAS Phased-Array Beamforming, 534	
11.6	Generic PWAS Phased-Array Formulation, 546	
11.7	2-D Planar PWAS Phased Array Studies, 553	
11.8	The 2-D Embedded Ultrasonic Structural Radar (2D-EUSR), 560	
11.9	Damage Detection Experiments Using Rectangular PWAS Array, 567	
11.10	Phased Array Analysis Using Fourier Transform Methods, 574	
11.11	Summary and Conclusions, 586	
11.12	Problems and Exercises, 587	
12	SIGNAL PROCESSING AND PATTERN RECOGNITION FOR PWAS-BASED STRUCTURAL HEALTH MONITORING	589
12.1	Introduction, 589	
12.2	From Fourier Transform to Short-Time Fourier Transform, 590	
12.3	Wavelet Analysis, 597	
12.4	State-of-the-Art Damage Identification and Pattern Recognition for Structural Health Monitoring, 617	
12.5	Neural Networks, 621	
12.6	Features Extractors, 632	

- 12.7 Case Study: E/M Impedance Spectrum for Circular Plates of Various Damage Levels, 634
- 12.8 Summary and Conclusions, 655
- 12.9 Problems and Exercises, 656

APPENDIX A MATHEMATICAL PREREQUISITES 657

- A.1 Fourier Analysis, 657
- A.2 Sampling Theory, 668
- A.3 Convolution, 670
- A.4 Hilbert Transform, 672
- A.5 Correlation Method, 675
- A.6 Time Averaged Product of Two Harmonic Variables, 677
- A.7 Harmonic and Bessel Functions, 679

APPENDIX B ELASTICITY NOTATIONS AND EQUATIONS 685

- B.1 Basic Notations, 685
- B.2 3-D Strain–Displacement Relations, 686
- B.3 Dilatation and Rotation, 687
- B.4 3-D Stress–Strain Relations in Engineering Constants, 688
- B.5 3-D Stress–Strain Relations in Lamé Constants, 689
- B.6 3-D Stress–Displacement Relations, 690
- B.7 3-D Equations of Motion, 690
- B.8 Traction, 691
- B.9 3-D Governing Equations—Navier Equations, 691
- B.10 2-D Elasticity, 692
- B.11 Polar Coordinates, 693
- B.12 Cylindrical Coordinates, 694
- B.13 Spherical Coordinates, 696

BIBLIOGRAPHY 699

INDEX 711

1

INTRODUCTION

1.1 STRUCTURAL HEALTH MONITORING PRINCIPLES AND CONCEPTS

Structural health monitoring (SHM) is an area of growing interest and worthy of new and innovative approaches. The United States spends more than \$200 billion each year on the maintenance of plant, equipment, and facilities. Maintenance and repairs represents about a quarter of commercial aircraft operating costs. Out of approximately 576 600 bridges in the US national inventory, about a third are either ‘structurally deficient’ and in need of repairs, or ‘functionally obsolete’ and in need of replacement. The mounting costs associated with the aging infrastructure have become an on-going concern. Structural health monitoring systems installed on the aging infrastructure could ensure increased safety and reliability.

Structural health monitoring is an area of great technical and scientific interests. The increasing age of our existing infrastructure makes the cost of maintenance and repairs a growing concern. Structural health monitoring may alleviate this by replacing scheduled maintenance with as-needed maintenance, thus saving the cost of unnecessary maintenance, on one hand, and preventing unscheduled maintenance, on the other hand. For new structures, the inclusion of structural health monitoring sensors and systems from the design stage is likely to greatly reduce the life-cycle cost.

Structural health monitoring is an emerging research area with multiple applications. Structural health monitoring assesses the state of structural health and, through appropriate data processing and interpretation, may predict the remaining life of the structure. Many aerospace and civil infrastructure systems are at or beyond their design life; however, it is envisioned that they will remain in service for an extended period. SHM is one of the enabling technologies that will make this possible. It addresses the problem of aging structures, which is a major concern of the engineering community. SHM allows condition-based maintenance (CBM) inspection instead of schedule-driven inspections. Another potential SHM application is in new systems; that is, by embedding SHM sensors and associate sensory systems into a new structure, the design paradigm can be changed and considerable savings in weight, size, and cost can be achieved. A schematic representation of a generic SHM system is shown in Fig. 1.1.

Structural health monitoring can be performed in two main ways: (a) passive SHM; and (b) active SHM. *Passive SHM* is mainly concerned with measuring various operational parameters and then inferring the state of structural health from these parameters. For example, one could monitor the flight parameters of an aircraft (air speed, air turbulence,

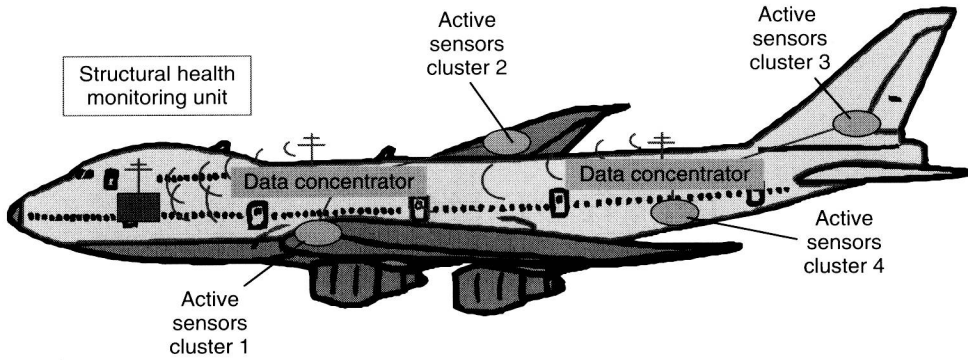


FIGURE 1.1 Schematic representation of a generic SHM systems consisting of active sensors, data concentrators, wireless communication, and SHM central unit.

g-factors, vibration levels, stresses in critical locations, etc.) and then use the aircraft design algorithms to infer how much of the aircraft useful life has been used up and how much is expected to remain. Passive SHM is useful, but it does not directly address the crux of the problem, i.e., it does not directly examine if the structure has been damaged or not. In contrast, *active SHM* is concerned with directly assessing the state of structural health by trying to detect the presence and extent of structural damage. In this respect, active SHM approach is similar with the approach taken by nondestructive evaluation (NDE) methodologies, only that active SHM takes it one-step further: active SHM attempts to develop damage detection sensors that can be permanently installed on the structure and monitoring methods that can provide on demand a structural health bulletin. Recently, damage detection through guided-wave NDE has gained extensive attraction. Guided waves (e.g., Lamb waves in plates) are elastic perturbations that can propagate for long distances in thin-wall structures with very little amplitude loss. In Lamb-wave NDE, the number of sensors required to monitor a structure can be significantly reduced. The potential also exist of using phased array techniques that use Lamb waves to scan large areas of the structure from a single location. However, one of the major limitations in the path of transitioning Lamb-wave NDE techniques into SHM methodologies has been the size and cost of the conventional NDE transducers, which are rather bulky and expensive. The permanent installation of conventional NDE transducers onto a structure is not feasible, especially when weight and cost are at a premium such as in the aerospace applications. Recently emerged *piezoelectric wafer active sensors* (PWAS) have the potential to improve significantly structural health monitoring, damage detection, and nondestructive evaluation. PWAS are small, lightweight, inexpensive, and can be produced in different geometries. PWAS can be bonded onto the structural surface, can be mounted inside built-up structures, and can be even embedded between the structural and nonstructural layers of a complete construction. Studies are also being performed to embed PWAS between the structural layers of composite materials, though the associated issues of durability and damage tolerance has still to be overcome.

Structural damage detection with PWAS can be performed using several methods: (a) *wave propagation*, (b) *frequency response transfer function*, or (c) *electromechanical (E/M) impedance*. Other methods of using PWAS for SHM are still emerging. However, the modeling and characterization of Lamb-wave generation and sensing using surface-bonded or embedded PWAS for SHM has still a long way to go. Also insufficiently advanced are reliable damage metrics that can assess the state of structural health with

confidence and trust. The Lamb-wave-based damage detection techniques using structurally integrated PWAS for SHM is still in its formative years. When SHM systems are being developed, it is often found that little mathematical basis is provided for the choice of the various testing parameters involved such as transducer geometry, dimensions, location and materials, excitation frequency, bandwidth, etc.

Admittedly, the field of structural health monitoring is very vast. A variety of sensors, methods, and data reduction techniques can be used to achieve the common goal of asking the structure ‘how it feels’ and determining the state of its ‘health’, i.e., structural integrity, damage presence (if any), and remaining life. Attempting to give an encyclopedic coverage of all such sensors, methods, and techniques is not what this book intends to do. Rather, this book intends to present an integrated approach to SHM using as a case study the PWAS and then taking the reader through a step-by-step presentation of how these sensors can be used to detect and quantify the presence of damage in a given structure. In this process, the book goes from simple to complex, from the modeling and testing of simple laboratory specimens to evaluation of large, realistic structures. The book can be used as a textbook in the classroom, as a self-teaching text for technical specialists interested in entering this new field, or a reference monograph for practicing experts using active SHM methods.

1.2 STRUCTURAL FRACTURE AND FAILURE

1.2.1 REVIEW OF LINEAR ELASTIC FRACTURE MECHANICS PRINCIPLES

The stress intensity factor at a crack tip has the general expression

$$K(\sigma, a) = C\sigma\sqrt{\pi a} \quad (1)$$

where σ is the applied stress, a is the crack length, and C is a constant depending on the specimen geometry and loading distribution. It is remarkable that the stress intensity factor increases not only with the applied stress, σ , but also with the crack length, a . As the crack grows, the stress intensity factor also grows. If the crack grows too much, a critical state is achieved when the crack growth becomes rapid and uncontrollable. The value of K associated with rapid crack extension is called the *critical stress intensity factor* K_c . For a given material, the onset of rapid crack extension always occurs at the same stress intensity value, K_c . For different specimens, having different initial crack lengths and geometries, the stress level, σ , at which rapid crack extension occurs, may be different. However, the K_c value will always be the same. Therefore, K_c is a property of the material. Thus, the condition for fracture to occur is that the local stress intensity factor $K(\sigma, a)$ exceeds the value K_c , i.e.,

$$K(\sigma, a) \geq K_c \quad (2)$$

We see that K_c provides a single-parameter fracture criterion that allows the prediction of fracture. Although the detailed calculation of $K(\sigma, a)$ and determination of K_c may be difficult in some cases, the general concept of using K_c to predict brittle fracture remains nonetheless applicable. The K_c concept can also be extended to materials that possess some limited ductility, such as high-strength metals. In this case, the $K(\sigma, a)$ expression (1) is modified to account for a crack-tip plastic zone, r_y , such that

$$K(\sigma, a) = C\sigma\sqrt{\pi(a + r_y)} \quad (3)$$

where the maximum value of r_Y can be estimated as

$$r_{Y\sigma} = \frac{1}{2\pi} \sqrt{\frac{K_c}{Y}} \quad (\text{plane stress}) \quad (4)$$

$$r_{Y\sigma} = \frac{1}{6\pi} \sqrt{\frac{K_c}{Y}} \quad (\text{plane strain}) \quad (5)$$

In studying the material behavior, one finds that the plane strain conditions give the lowest value of K_c , whereas the plane stress conditions can give K_c values that may range from two to ten times higher. This effect is connected with the degree of constraint imposed upon the material. Materials with higher constraint effects have a lower K_c value. The plane strain condition is the condition with most constraint. The plane strain K_c is also called the *fracture toughness* K_{Ic} of the material. Standard test methods exist for determining the material fracture-toughness value. When used in design, fracture-toughness criteria gives a larger margin of safety than elastic-plastic fracture mechanics methods such as (a) crack opening displacement (COD) methods; (b) R-curve methods; (c) J-integral methods. However, the fracture toughness approach is more conservative: it is safer, but heavier. For a complete design analysis, the designer should consider, in most cases, both conditions: (a) the possibility of failure by brittle fracture; and (b) the possibility of failure by ductile yielding.

1.2.2 FRACTURE MECHANICS APPROACH TO CRACK PROPAGATION

The concepts of linear fracture mechanics can be employed to analyze a given structure and predict the crack size that will propagate spontaneously to failure under the specified loading. This critical crack size can be determined from the critical stress intensity factor as defined in Eq. (3). A fatigue crack that has been initiated by cyclic loading, or other damage mechanism, may be expected to grow under sustained cyclic loading until it reaches a critical size beyond which will propagate rapidly to catastrophic failure. Typically, the time taken by a given crack damage to grow to a critical size represents a significant portion of the operational life of the structure. In assessing the useful life of a structure, several things are needed such as:

- understanding of the crack-initiation mechanism
- definition of the critical crack size, beyond which the crack propagates catastrophically
- understanding the crack-growth mechanism that makes a subcritical crack propagate and expand to the critical crack size.

Experiments of crack length growth with number of cycles for various cyclic-load values have indicated that a high value of the cyclic load induces a much more rapid crack growth than a lower value (Collins, 1993). It has been found that crack growth phenomenon has several distinct regions (Fig. 1.2):

- (i) An initial region in which the crack growth is very slow
- (ii) A linear region in which the crack growth is proportional with the number of cycles
- (iii) A nonlinear region in which the log of the crack growth rate is proportional with the log of the number of cycles.

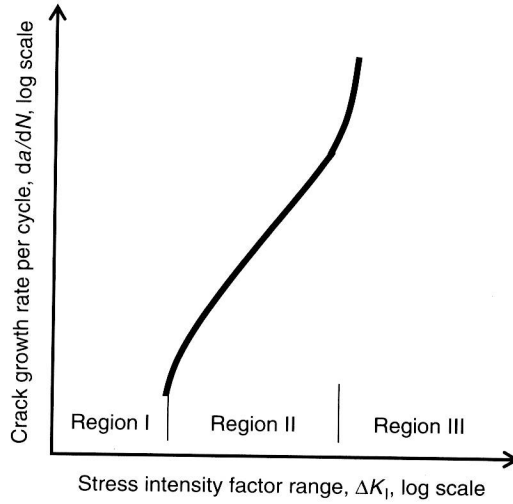


FIGURE 1.2 Schematic representation of fatigue crack growth in metallic materials.

In analyzing fatigue crack growth, Paris and Erdogan (1963) determined that the fatigue crack-growth rate depends on the alternating stress and crack length:

$$\frac{da}{dN} = f(\Delta\sigma, a, C) \quad (6)$$

where $\Delta\sigma$ is the peak-to-peak range of the cyclic stress, a is the crack length, and C is a parameter that depends on mean load, material properties, and other secondary variables.

In view of Eq. (1), it seems appropriate to assume that the crack-growth rate will depend on the cyclic stress intensity factor, ΔK , i.e.,

$$\frac{da}{dN} = g(\Delta K) \quad (7)$$

where ΔK is the peak-to-peak range of the cyclic stress intensity factor. Experiments have shown that, for various stress levels and various crack lengths, the data points seem to follow a common law when plotted as crack-growth rate versus stress intensity factor (Collins, 1993). This remarkable behavior came to be known as 'Paris law'; its representation corresponds to the middle portion of the curve shown in Fig. 1.2. Fatigue-crack growth-rate laws have been reported for a wide variety of engineering materials. As middle portion of the curve in Fig. 1.2 is linear on log-log scale, the corresponding Eq. (7) can be written as:

$$\frac{da}{dN} = C_{EP}(\Delta K)^n \quad (8)$$

where n is the slope of the log-log line, and C_{EP} is an empirical parameter that depends upon material properties, test frequency, mean load, and some secondary variables. If the parameter C_{EP} and n are known, then one can predict how much a crack has grown after N cycles, i.e.,

$$a(N) = a_0 + \int_1^N C_{EP}(\Delta K)^n dN \quad (9)$$

where a_0 is the initial crack length.

Paris law represents well the middle portion of the curve in Fig. 1.2. However, the complete crack-growth behavior has three separate phases:

- (1) Crack nucleation
- (2) Steady-state regime of linear crack growth on the log-log scale
- (3) Transition to the unstable regime of rapid crack extension and fracture.

Such a situation is depicted in Fig. 1.2, where Region I corresponds to the crack nucleation phase, Region II to linear growth, and Region III to transition to the unstable regime. Threshold values for ΔK that delineate one region from the other seem to exist. As shown in Fig. 1.2, the locations of these regions in terms of stress intensity factor vary significantly from one material to another.

Paris law is widely used in engineering practice. Further studies have revealed several factors that also need to be considered when applying Paris law to engineering problems. Some of these factors are

- Influence of cyclic stress ratio on the threshold value of ΔK
- Difference between constant-amplitude tests and spectrum loading
- Effect of maximum stress on spectrum loading
- Retardation and acceleration effects due to overloads.

The influence of the stress ratio and threshold have been incorporated in the modified Paris law (Hartman and Schijve, 1970)

$$\frac{da}{dN} = \frac{C_{HS}(\Delta K - \Delta K_{TH})^m}{(1-R)K_c - \Delta K} \quad (10)$$

where R is the stress ratio $\sigma_{\max}/\sigma_{\min}$, K_c is the fracture toughness for unstable crack growth under monotonic loading, ΔK_{TH} is the threshold cyclic stress intensity factor for fatigue propagation, and C_{HS} is an empirical parameter.

The difference between constant-amplitude loading and spectrum loading has been shown to depend on the maximum stress value. If the maximum stress is held at the same values in both constant-amplitude and spectrum loading, then the crack growth rates seem to follow the same law. However, if the maximum stress is allowed to vary, the spectrum loading results seem to depend strongly on the sequence in which the loading cycles are applied, with the overall crack growth being significantly higher for spectrum loading than for constant-amplitude loading (McMillan and Pelloux, 1967). The retardation effects due to overloads have been reported by several investigators as evidence of the *interaction effect* whereby fatigue damage and crack extension depend on preceding cyclic-load history. An interaction of considerable interest is the *retardation* of crack growth due to the application of occasional cycles of crack-opening overload. Retardation is characterized by a period of reduced crack-growth rate following the application of a peak load higher than the subsequent peak. The retardation has been explained by the inference that the overload will induce yield at the crack tip and will produce a zone of local plastic deformation in the crack-tip vicinity. When the overload is removed, the surrounding material forces the yielded zone into a state of residual compression that tends to inhibit the crack growth under the subsequent loads of lower value. The crack-growth rate will remain smaller until the growing crack has traversed the overload yield zone, when it returns to the normal value. Crack-growth *acceleration*,

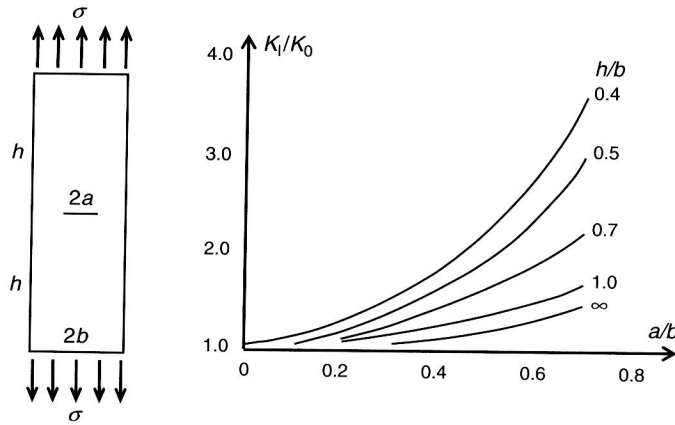


FIGURE 1.3 Plate (length = $2h$, width = $2b$), containing a central crack length of $2a$. Tensile stress σ acts in the longitudinal direction.

on the other hand, may occur after crack-closing overloads. In this case, the overload yield zone will produce residual tension stresses, which add to the subsequent loading and result in crack-growth acceleration.

For simple geometries, the stress intensity factor can be predicted analytically. Such predictions have been confirmed by extensive experimental testing; look-up tables and graphs have been made available for design usage. For example, a rectangular specimen with a crack in the middle has stress intensity factor for mode I cracking given by

$$K_I = \beta \sigma \sqrt{\pi a} \quad (11)$$

where σ is the applied tensile stress, a is half of the crack length, and $\beta = K_I/K_0$. The term K_0 represents the ideal stress intensity factor corresponding to an infinite plate with a single crack in the center. The parameter β represents the effect of having a plate of finite dimensions, i.e., the changes in the elastic field due to the plate boundaries not being infinitely far from the crack (Fig. 1.3). The value of the parameter β for a large variety of specimen geometries can be found in the literature.

1.3 IMPROVED DIAGNOSIS AND PROGNOSIS THROUGH STRUCTURAL HEALTH MONITORING

1.3.1 FRACTURE CONTROL THROUGH NDI/NDE

In-service inspection procedures play a major role in the fail-safe concept. Structural regions and elements are classified with respect to required nondestructive inspection (NDI) and NDE sensitivity. Inspection intervals are established on the basis of crack growth information assuming a specified initial flaw size and a 'detectable' crack size, a_{det} , the latter depending on the level of available NDI/NDE procedure and equipment. Cracks larger than a_{det} are presumed to be discovered and repaired. The inspection

intervals must be such that an undetected flaw will not grow to critical size before the next inspection. The assumptions used in the establishment of inspection intervals are

- All critical points are checked at every inspection
- Cracks larger than a_{det} are all found during the inspection
- Inspections are performed on schedule
- Inspection techniques are truly nondamaging.

In practice, these assumptions are sometimes violated during infield operations, or are impossible to fulfill. For example, many inspections that require extensive disassembly for access may result in flaw nucleation induced by the disassembly/reassembly process. Some large aircraft can have as many as 22 000 critical fastener holes in the lower wing alone (Rich and Cartwright, 1977). Complete inspection of such a large number of sites is not only tedious and time consuming, but also subject to error born of the boredom of inspecting 20 000 holes with no serious problems, only to miss one hole with a serious crack (sometimes called the 'rogue' crack). Nonetheless, the use of NDI/NDE techniques and the establishment of appropriate inspection intervals have progressed considerably. Recent developments include automated scanning systems and pattern-recognition method that relieve the operator of the attention consuming tedious decision making in routine situations and allow the human attention to be concentrated on truly difficult cases. Nevertheless, the current practice of scheduled NDI/NDE inspections leaves much to be desired.

1.3.2 DAMAGE TOLERANCE, FRACTURE CONTROL AND LIFE-CYCLE PROGNOSIS

A *damage tolerant* structure has a design configuration that minimizes the loss of aircraft due to the propagation of undetected flaws, cracks, and other damage. To produce a damage-tolerant structure, two design objectives must be met:

- (1) Controlled safe flaw growth, or safe life with cracks
- (2) Positive damage containment, i.e., a safe remaining (residual) strength.

These two objectives must be simultaneously met in a judicious combination that ensures effective fracture control. Damage-tolerant design and fracture control includes the following:

- (i) Use of fracture-resistant materials and manufacturing processes
- (ii) Design for inspectability
- (iii) Use of damage-tolerant structural configurations such as multiple load paths or crack stoppers (Fig. 1.4).

In the application of fracture control principles, the basic assumption is that flaws do exist even in new structures and that they may go undetected. Hence, any member in the structure must have a *safe life* even when cracks are present. In addition, flight-critical components must be *fail-safe*. The concept of *safe life* implies the evaluation of the expected lifetime through margin-of-safety design and full-scale fatigue tests. The margin of safety is used to account for uncertainties and scatter. The concept of *fail-safe* assumes that flight-critical components cannot be allowed to fail, hence alternative load paths are

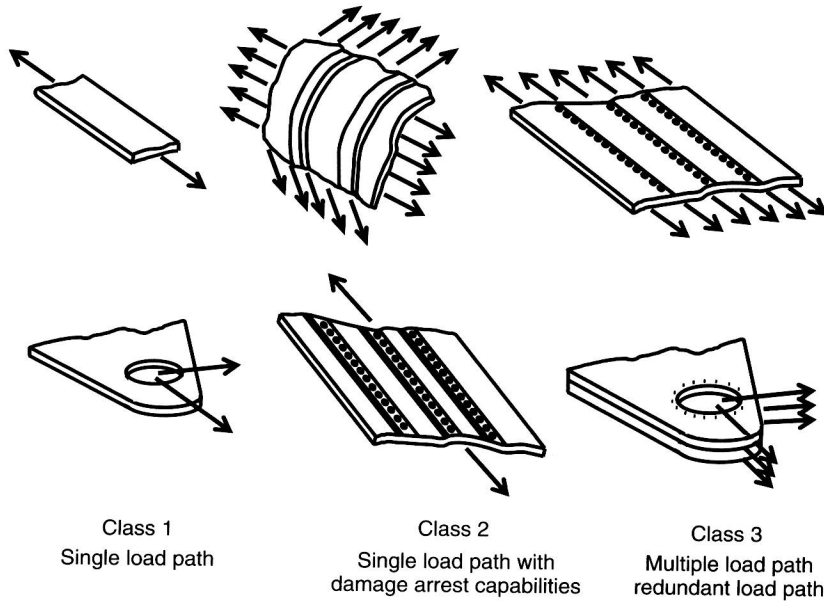


FIGURE 1.4 Structural types based on load path.

supplied through redundant components. These alternative load paths are assumed to be able to carry the load until the failure of the primary component is detected and a repair is made.

1.3.3 LIFE-CYCLE PROGNOSIS BASED ON FATIGUE TESTS

The estimated design life of an aircraft is based on full-scale fatigue testing of complete test articles under simulated fatigue loading. The benefits of full-scale fatigue testing include:

- Discover fatigue critical elements and design deficiencies
- Determine time intervals to detectable cracking
- Collect data on crack propagation
- Determine remaining safe life with cracks
- Determine residual strength
- Establish proper inspection intervals
- Develop repair methods.

The structural life proved through simulation test should be longer by a factor from two to four than the design life. Full-scale fatigue testing should be continued over the long term such that fatigue failures in the test article will stay ahead of the fleet experience by enough time to permit the redesign and installation of whatever modifications are required to prevent catastrophic fleet failures. However, full-scale fatigue testing of an article such as a newly designed aircraft is extremely expensive. In addition, the current aircraft in our fleets have exceeded the design fatigue life, and hence are no longer covered by the full-scale fatigue testing done several decades ago.